# Simultaneous two-dimensional nanometric-scale position monitoring by probing a two-dimensional photonic crystal plate

Kuei-Chu Hsu*[a], Chii-Chang Chen[a], Chia-Hua Chan[a], Pei-Fang Chung[b], Yinchieh Lai[b]
[a]Department of Optics and Photonics, National Central University, 320 Jhung-Li, Taiwan;
[b]Department of Photonics and Institute of Electro-Optical Engineering, National Chiao Tung University, 300 Hsinchu, Taiwan

## ABSTRACT

Simultaneous two-dimensional nanometric-scale position monitoring can be achieved in a simple interferometric setup by real-time probing a hexagonal photonic crystal glass substrate. The minimum detectable translational movement is determined by the period of photonic crystal array, and can be as high as 8 nm in the present work.
**Keywords:** Times Roman, image area, acronyms, references

## 1. INTRODUCTION

The recent rapid progress of nanophotonics research urgently requires the technique to control the position of objects with nanometric precision. The nanometric-scale position monitoring method in the literature mainly combines the delicate optical method with mechanical tuning element. (1-7) Though the best detection abilities can reach nanoscale, the above methods suffering from not only the limitation of detection length but also the lack of simultaneous two- or three-dimensional displacement measurement in a simple setup.

In this work, a simple way to achieve simultaneous two-dimensional nanometric-scale position monitoring is proposed that can in principle attain the nanometric-scale accuracy of position reading in both orthogonal moving directions, and this method also has the potential to reach simultaneous two-dimensional long-distance displacement measurement and small rotation detection. The real-time interferometric position monitoring method is based on our previous work. [3] To real-time monitor the two-dimensional translational movement in nanometric-scale, an optical imaging system is built by probing a hexagonal photonic crystal glass (HPCG) with a 633-nm He-Ne laser beam. The translation movements in both directions are recorded in the phase term of the fields of the diffracted six spots. Carefully align the first-order two spots and the zero-order spot to form chessboard-like interference pattern on the CCD camera, the individual nanometric-scale movement information can be determined by the phase change of the chessboard-like interference pattern before and after moving.

## 2. THEOREM AND EXPERIMENT

The real-time two-dimensional position monitoring with nanometric-scale is achieved via the application of position movement along the x and y axis on the imaging system of the transparent hexagonal-arranged photonic crystal array glass substrate. Figure 1 displays the diffraction pattern of a HPCG located at the focal point of a converging lens with 125-mm-long focal length. A 633-nm He-Ne laser beam is focused onto the HPCG, and the optical diffraction pattern is projected on the screen. The center spot is the zero-order beam, and the surrounding six spots are the first-order diffraction beams. When the sample rotates, the six-spot diffracted image rotates as well.

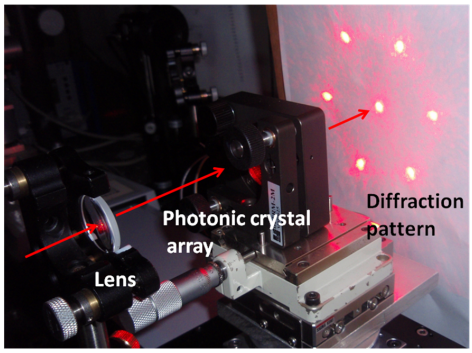


Photonic and Phononic Crystal Materials and Devices X, edited by Ali Adibi, Shawn-Yu Lin, Axel Scherer,
Proc. of SPIE Vol. 7609, 76091J · © 2010 SPIE · CCC code: 0277-786X/10/$18 · doi: 10.1117/12.839187

Figure 1. Diffraction pattern of a photonic crystal array glass.

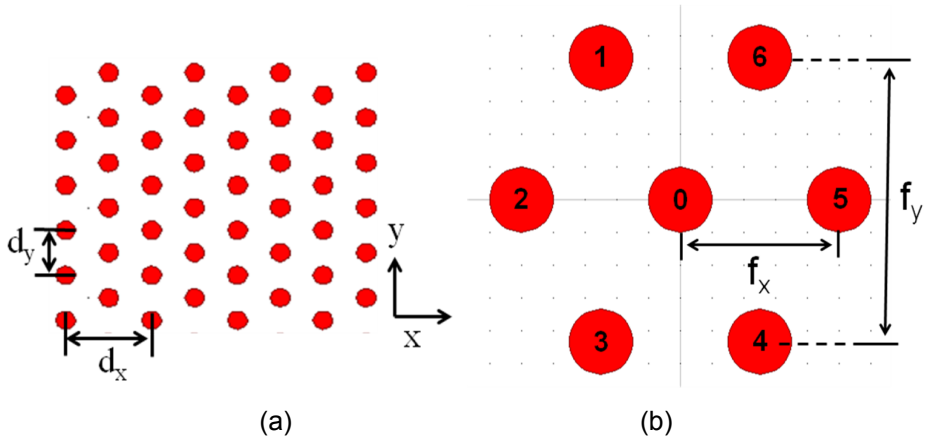


Figure 2. (a) Sketches of a hexagonal-lattice glass and (b) the corresponding first-order diffracted spots.

Figure 2 (a) and 2(b) plots the sketch of HPCG arranged in a hexagonal geometry and its first-order diffraction pattern. The transmittance of the HPCG in Fig. 2(a) can be written in terms of convolution

$$t(x,y) = g(x,y) \otimes [comb(\frac{x}{d_x})comb(\frac{y}{d_y}) + comb(\frac{x}{d_x} - \frac{1}{2})comb(\frac{y}{d_y} - \frac{1}{2})], \quad (1)$$

where t(x,y) denotes transmittance of the photonic crystal array, dx and dy are the periods of the array along the x and y directions, and g(x,y) is the transmittance of one unit cell. The Fraunhofer diffraction pattern of a 2D hexagonal array is the Fourier spectrum of the hexagonal structure. The diffracted field can be expressed in the following Fourier series expansion:

$$u_z(x,y) = \sum_{m,n} G(f_x - \frac{n}{d_x}, f_y - \frac{m}{d_y}), . \quad (2)$$

Equation 2 shows the field distribution uz(x,y) along z direction, fx and fy are the spatial frequencies of the image along the x and y directions, and G is the Fourier transform of g(x, y). When the translation in position applied on the array, the phase term of the imaging field carry the position movement information. If the two-dimensional translation x1 and y1 are simultaneously applied, the diffraction field uz'(x,y) can be shown in Eq. 3,

$$u_z'(x - x_1, y - y_1) = u_z(x,y)e^{i2\pi f_x x_1}e^{i2\pi f_y y_1} = u_{0z}(x,y)e^{i\delta_0} + u_{1z}(x,y)e^{i\delta_1} + u_{2z}(x,y)e^{i\delta_2} + \cdots, \quad (3)$$

where u0z(x,y), u1z(x,y) and u2z(x,y) are the fields of spot 0, spot 1 and spot 2 denoted in Fig. 2(b) and δ0, δ1 and δ2 are the phase difference of spot 0, spot 1 and spot 2 before and after translational movement. Though the diffracted spots remain the same configuration, the movement information is recorded in the phase term of the fields. Separately take the

diffracted spot 1 and spot 2 to interfere with the zero-order spot 0, the recorded phase information $\delta_1$ and $\delta_2$ can be revealed in the phase of the interference pattern, as shown in Eq. 4.

$$\boldsymbol{I}_{\text{int}} = \boldsymbol{I}_0 + \boldsymbol{I}_0 \cos(\boldsymbol{\theta}_0 + \boldsymbol{\delta}_{1,2}). \tag{4}$$

The $I_{int}$ and $I_0$ respectively represent the intensity distribution of the interference pattern and the dc term of the interference pattern, and θ0 denotes the initial phase of the interference field. The interference pattern Iint is processed by the Fourier transform to obtain the corresponding spatial frequency spectrum. The spectrum is then filtered to keep only the positive frequency part and is inverse-Fourier-transformed back to the original domain. The phase δ1 and δ1 can then be identified by taking the arg of the processed data, thus the phase change of the interference pattern can be inferred from monitoring the phase difference δ1 and δ2. Once the phase δ1 and δ1 are determined, the movement x1 and y1 can be decided.

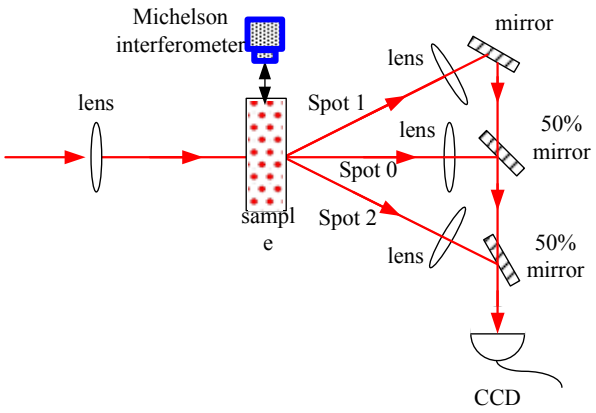


(a)

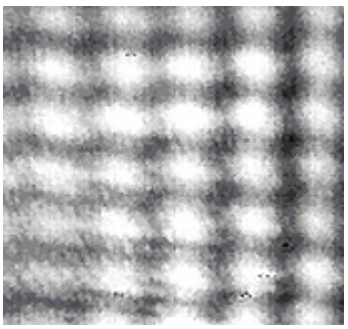

(b)

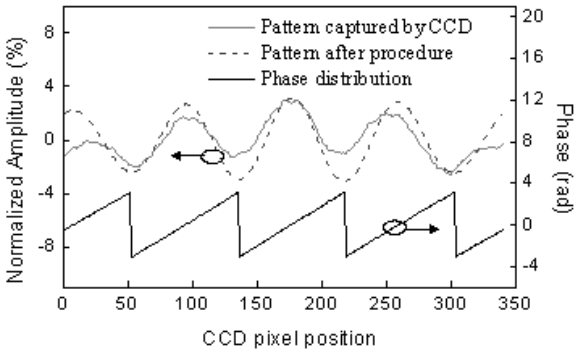


(c)

Figure 3. (a) Schematic diagram of experimental setup. (b) chessboard-like interference pattern. (c) Typical 1D interference pattern captured by CCD, the pattern after procedure and the calculated phase distribution.

Transparent HPCG sample is prepared by etching the glass substrate from deposing a tightly-align polymer sphere monolayer, and surface corrugated plane with hexagonal geometry thus formed. [8] The sample can be highly uniform over inch square. To build the whole position monitoring system, the experimental setup is plotted as Fig. 3 (a). A single-

polarization 633-nm He-Ne laser beam is focused onto the photonic crystal array with a spherical lens of 125-mm focal length, and the first-order diffraction spots are generated as shown in Fig. 2(b). Zero-order spot 0 and first-order spot 1 and spot 2 are combined at the beam combiners with interference angles of θ1 and θ2 in orthogonal directions, therefore, the chessboard-like interference pattern are formed. A 440×480 monochrome CCD camera with a pixel width of 7.15-μm is utilized to record the chessboard-like interference pattern produced by spots 0, 1 and 2, as displayed in Fig. 3(b). One axial direction of the two-dimensional intensity distribution of the interference fringe is recorded on the CCD camera to illustrate the imaging processing algorithm. Figure 3(c) shows the typically resulted periodic pattern along the x-axis captured by the CCD camera (grey solid line), the pattern after the filtering+taking-real-part procedure (grey dotted line) and the obtained phase distribution by taking the arg of the filtered data (bold solid line). [9]

To test the nanometric-scale movement detection algorithm, the system is implemented with the LabVIEW software for automatically controlling the whole position monitoring process. The one dimensional position reading is executed firstly. The sample is mounted on a translation stage comprised of a linear motor stage and a piezoelectric translator (PZT) stage with sub-nm position resolution. The accurate movement of one period is achieved by shifting the translation stage to an approximate distance and then iteratively fine-tuning the PZT stage to match the phase distribution of the interference pattern on CCD camera. The iteration process terminates when the phase distribution obtained in this step matches that of last step. The accurate amount of movement is recorded by the Michelson interferometer. Figure 4 displays the period number versus the average movement distance with the sample placed 0° from moving axis (as the geometry arranged in Fig. 2(a)) and rotate 60° with z-axis from Fig. 2(a). The sample period is approximately 1357 nm. The period should keep the same value when the sample rotates 60 degree for its geometric symmetry, and Fig. 4 indicates reasonable data trend as expected.

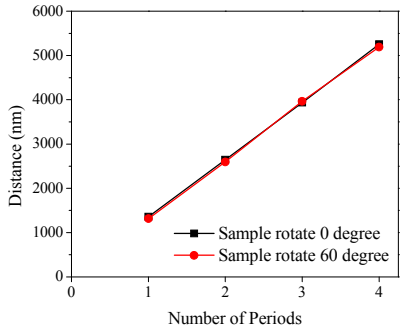


Figure 4. Number of period versus translational distance for HPCG crystal axis placed at 0° and 60°.

We further investigate one-dimensional position monitoring accuracy by introducing different phase shift respect to one period. Table 1 lists the statistical data for average displacement and standard deviation of total 50 measurements per phase shift. In our preliminary experimental setup, the position monitoring accuracy of the whole system is better than 1.8 nm, which means the accuracy of the position-seeking feedback control loop is set to be 0.5 degree of the array period. From Tab. 1, the minimum detectable translational movement can be as high as 8 nm for 2 degree phase shift respect to one period of HPCG sample.

Table 1. One-dimensional position monitoring statistics data according to the amount of phase shifts respect to one period.

| | Phase shift (degree) | | | | |
|---|---|---|---|---|---|
| | 2 | 5 | 60 | 180 | 360 |
| Average displacement (nm) | 8.12 | 19.06 | 439.67 | 664.51 | 1357.51 |
| Standard deviation (nm) | 0.94 | 1.65 | 5.70 | 12.63 | 18.03 |

The minimum detectable translational movement and position accuracy and resolution of the whole system are mainly limited by the wavelength of the probe laser beam and the period of the photonic crystal array, and can be as high as nanometric-scale for long distance position monitoring since the sample can be highly uniform over large scale. Two-dimensional simultaneous detection can be carried out according to the same algorithm, and is under progress now. Besides, the rotation of the sample with respect to moving plane can result in the rotation of the diffracted spots configuration. Thus this setup possesses the potential to further detect the small rotation angle in addition to the simultaneous two-dimensional position monitoring capability. Deeper investigation on the translational and rotational detection based on the proposed setup will be presented in the Conference.

## 3. CONCLUSIONS

Real-time interferometric two-dimensional nanometric-scale position monitoring is proposed via the application of translational movement on the imaging system of a hexagonal photonic crystal array. The position accuracy is mainly determined by the period of photonic crystal array, and can be as high as 8 nm in the present work. The proposed setup is capable for simultaneous two-dimensional translational movement detection as well as rotation detection.

## REFERENCES


1. E.-T. Hwu, S.-K. Hung, C.-W. Yang, and I.-S. Hwang, "Simultaneous detection of translational and angular displacements of micromachined elements," App. Phys. Lett. **91**, 221908 (2007).
*2*. B. Van Gorp, A. G. Onaran, and F. L. Degertekin, "Integrated dual grating method for extended range interferometric displacement detection in probe microscopy," App. Phys. Lett. **91,** 083101 (2007).
3. Fan Chen, Zhuangqi Cao, Qishun Shen, Xiaoxu Deng, Biming Duan, Wen Yuan, Minghuang Sang and Sgengqian Wang, "Nanoscale displacement measurement in a variable-air-gap optical waveguide," App. Phys. Lett. **88,** 161111 (2007).
4. Wook Lee, Neal A. Hall, and F. Levent Degertekin, "A grating-assisted resonant-cavity-enhanced optical displacement detection method for micromachined sensors," App. Phys. Lett. **85,** 3032-3034 (2004).
5. Onur Ferhanoglu, M. Fatih Toy, and Hakan Urey, "Two-wavelength grating interferometry for MEMS seneors," IEEE Photon. Technol. Lett. **19,** 1895-1897 (2007).
6. Dalip Singh Mehta, Satish Kumar Dubey, Chandra Shakher, and Mitsuo Takeda, "Two-wavelength Talbot effect and its application for three-dimensional step-height measurement," Appl. Opt. **45,** 7602-7609 (2006).
7. Tianyi Yu, Honggen Li, Zhuangqi Cao, Yi Wang, Qishun Shen, and Ying He, "Oscillating wave displacement sensor using the enhanced Goos-Hanchen effect in a symmetrical metal-cladding optical waveguide," Opt. Lett. **33,** 1001-1003 (2008).
8. Chia-Hua Chan, Chia-Hung Hou, Chih-Kai Huang, Tsing-Jen Chen, Shao-Ze Tseng, Hung-Ta Chien,Cheng-Huang Kuo, Kuo-Huang Hsieh, Yen-Ling Tsai, Kuei-Chu Hsu, and Chii-Chang Chen, "Patterning periodical motif on substrates using monolayer of microspheres: application in GaN light-emitting diodes," Jpn. J. Appl. Phys. **48,** 020212 (2009).
9. Kuei-Chu Hsu, Lih-Gen Sheu, Kai-Ping Chuang, Shu-Hui Chang and Yinchieh Lai, "Fiber Bragg grating sequential UV-writing method with real-time interferometric side-diffraction position monitoring," Opt. Express **13,** 3795-3801 (2005).